

Article

Isolation and Characterization of Plasma-Derived Exosomes from the Marine Fish Rock Bream (*Oplegnathus fasciatus*) by Two Isolation Techniques

Chamilani Nikapitiya, Eriyawala Hewage Thimira Thulshan Jayathilaka , Shan Lakmal Edirisinghe, Dinusha C. Rajapaksha, Withanage Prasadini Wasana, Jayasinghage Nirmani Chathurangika Jayasinghe and Mahanama De Zoysa * 

College of Veterinary Medicine, Chungnam National University, Daejeon 34134, Korea; chamilani14@cnu.ac.kr (C.N.); thimira.thulshan@o.cnu.ac.kr (E.H.T.T.J.); shanlakmal@o.cnu.ac.kr (S.L.E.); dinusharajapaksha@o.cnu.ac.kr (D.C.R.); wasanaprasadini@o.cnu.ac.kr (W.P.W.); nirmanijay@o.cnu.ac.kr (J.N.C.J.)
* Correspondence: mahanama@cnu.ac.kr



Citation: Nikapitiya, C.; Jayathilaka, E.H.T.T.; Edirisinghe, S.L.; Rajapaksha, D.C.; Wasana, W.P.; Jayasinghe, J.N.C.; De Zoysa, M. Isolation and Characterization of Plasma-Derived Exosomes from the Marine Fish Rock Bream (*Oplegnathus fasciatus*) by Two Isolation Techniques. *Fishes* **2022**, *7*, 36. <https://doi.org/10.3390/fishes7010036>

Academic Editor: Jesús L. Romalde

Received: 10 November 2021

Accepted: 26 January 2022

Published: 2 February 2022

Publisher's Note: MDPI stays neutral with regard to jurisdictional claims in published maps and institutional affiliations.



Copyright: © 2022 by the authors. Licensee MDPI, Basel, Switzerland. This article is an open access article distributed under the terms and conditions of the Creative Commons Attribution (CC BY) license (<https://creativecommons.org/licenses/by/4.0/>).

Abstract: Exosomes are important mediators of intercellular communication and modulate many physiological and pathological processes. Knowledge of secretion, content, and biological functions of fish exosomes during pathological infection is still scarce due to lack of suitable standardized isolation techniques. In this study, we aimed to isolate exosomes from the plasma of marine fish, rock bream (*Oplegnathus fasciatus*), by two isolation methods: differential ultracentrifugation (UC) and a commercial membrane affinity spin column technique (kit). Morphological and physicochemical characteristics of the isolated exosomes were determined by these two methods, and the efficiencies of the two methods were compared. Exosomes isolated by both methods were in the expected size range (30–200 nm) and had a characteristic cup-shape in transmission electron microscopy observation. Moreover, more intact exosomes were identified using the kit-based method than UC. Nanoparticle tracking analysis demonstrated a heterogeneous population of exosomes with a mean particle diameter of 114.6 ± 4.6 and 111.2 ± 2.2 nm by UC and a kit-based method, respectively. The particle concentration obtained by the kit method ($1.05 \times 10^{11} \pm 1.23 \times 10^{10}$ particles/mL) was 10-fold higher than that obtained by UC ($4.90 \times 10^{10} \pm 2.91 \times 10^9$ particles/mL). The kit method had a comparatively higher total protein yield (1.86 mg) and exosome protein recovery (0.55 mg/mL plasma). Immunoblotting analysis showed the presence of exosome marker proteins (CD81, CD63, and HSP90) in the exosomes isolated by both methods and suggests the existence of exosomes. However, the absence of cytotoxicity or adverse immune responses to fish and mammalian cells by the exosomes isolated by the UC procedure indicates its suitability for functional studies *in vitro*. Overall, our basic characterization results indicate that the kit-based method is more suitable for isolating high-purity exosomes from fish plasma, whereas UC has higher safety in terms of yielding exosomes with low toxicity. This study provides evidence for the existence of typical exosomes in rock beam plasma and facilitates the selection of an efficient exosome isolation procedure for future applications in disease diagnosis and exosome therapy as fish medicine.

Keywords: extracellular vesicles (EVs); fish exosomes; *Oplegnathus fasciatus*; rock bream; ultracentrifugation

1. Introduction

Exosomes are nano-sized (30–200 nm), membrane-bound, extracellular vesicles (EVs) secreted by various cell types that are capable of intercellular communication [1]. EVs are formed by inward budding of the lipid bilayer membrane during the maturation of these vesicles into multivesicular bodies in the endocytic pathway and are enriched with bioactive cargos (e.g., miRNA, mRNA, proteins, and lipids). Exosomes are distributed in a variety of body fluids, and owing to their wide range of functions in normal physiological

processes, as well as under pathological conditions, they are of wide scientific and clinical research interest [2,3]. The genetic and proteomic information derived from parent cells leads to exosomes being potential biomarkers for disease diagnosis and prognosis by non-invasive analysis of their molecular profiles [4]. The importance of exosomes in terms of having various beneficial roles in physiological processes, as well as detrimental roles in pathological processes in humans and other mammals has been widely discussed within the field of exosome research [5]. Fish exosome research is at a primitive stage, with few reported studies related to aquatic animals [6–12]. Analyzing body fluids in teleosts can deepen the understanding of exosomes with regard to their secretion into the extracellular fluids, such as plasma, and their biological functions. Moreover, in-depth research on fish exosomes will facilitate disease diagnosis and enhance the understanding of host–pathogen interactions and the role of EV/exosome cargos resulting from the expression of pathogen-derived factors in eliciting immune defence responses and immune regulatory mechanisms during viral and bacterial infections [9,13].

Rock bream (*Oplegnathus fasciatus*) aquaculture is greatly impacted by the rock bream iridovirus (RBIV), which belongs to the genus Megalocytivirus of the Iridoviridae family and causes significant mass mortality in the population [14,15]. Various immune response studies against the strongly pathogenic RBIV have been conducted at physiological and molecular levels via microarray, transcriptomic, and proteomic analyses at different organ levels [16]. It has been reported that teleost red blood cells (RBCs), which are nucleated and contain organelles in the cytoplasm, can produce immune responses against pathogens such as viruses. For instance, rainbow trout (*Oncorhynchus mykiss*) RBCs can elicit immune functions, such as cytokine production, leukocyte activation, and antigen presentation [17,18]. Recently, Jung et al. performed the proteomic profiling of RBCs from RBIV-infected rock bream fish and identified 318 proteins from RBIV-infected specimens that showed significantly altered expression in RBCs, comprising 183 upregulated (e.g., proteins related to antigen processing and presentation, apoptosis) and 135 downregulated (e.g., ISG15 antiviral mechanism pathway) proteins [16]. Although these findings collectively contribute to understanding the immune responses against RBIV pathogenesis, identification of the underlying mechanism of RBIV pathogenesis and host–pathogen interactions remain to be elucidated. We propose the use of exosomes and exosome-based immunotherapy as an attractive novel approach for RBIV diagnosis and for evoking immune responses against pathogens.

In this study, rock bream plasma-derived exosomes were isolated using two isolation methods: the conventional differential ultracentrifugation (UC) method and the commercially available, membrane affinity spin column-based, exoEasy Maxi kit, and compared the efficacy of the kit with that of UC based on the exosome yield, purity, and quantity. Exosomes were characterized based on their morphology, particle size, concentration, and zeta potential, and by immunoblotting-based, exosome-protein marker analysis. In order to identify the safety-related aspects of the isolated naive exosomes derived from rock bream plasma, *in vitro* toxicity and immune response analysis were conducted using the fathead minnow (FHM) fish epithelial cell line and the murine macrophage RAW 264.7 cell line. The findings of this study can facilitate the selection of further optimized procedures for exosome isolation in fish and of the desired downstream applications of exosomes, such as the development of biologically active agents (e.g., compounds for wound healing and those with anti-inflammatory and antimicrobial properties), potential drug delivery carriers (e.g., miRNA, peptide), and antigen carriers for vaccines.

2. Materials and Methods

2.1. Blood Collection and Plasma Isolation

Blood was collected from the caudal veins of five rock bream fish (500 ± 53 g) using a syringe containing 50 μ L of 0.5 M EDTA into BD Vacutainer Venous Blood Collection Tubes (cat. No. 367525, BD, Plymouth, United Kingdom) containing EDTA. For the plasma separation, the blood was kept at room temperature (RT; 25 °C) for 15 min, centrifuged at

2000× *g* at 20 °C for 10 min, and the supernatant comprising the upper plasma phase was carefully transferred to a new tube. The supernatant was re-centrifuged at 3000× *g* at 20 °C for 15 min and filtered through a 0.45 µm filter. The filtrate was either used immediately or aliquoted into 1.5 mL micro tubes and stored at −80 °C for further analysis. Isolation of exosomes by UC involved maintaining the collected blood at RT for 15 min and then eliminating the red blood cells and peripheral blood leukocytes by centrifugation at 480× *g* for 5 min at 20 °C. The supernatant was centrifuged at 2000× *g* for 10 min at 20 °C, and the upper plasma fraction was transferred to a tube and re-centrifuged at 2000× *g* for 10 min at 20 °C to remove cell debris. The supernatant (plasma) was collected and filtered through a 0.45 µm filter. The filtrate was either used immediately or aliquoted into 1.5 mL microtubes and stored at −80 °C for further analysis.

2.2. Plasma Exosome Isolation

Exosomes were isolated from the plasma samples by differential UC or the commercial kit. Purification of plasma exosomes by UC was performed according to methods described in previously published studies with a few modifications [7,19,20]. Pooled plasma (3.4 mL) was diluted to a 3:1 ratio with 1× phosphate-buffered saline (1× PBS; 0.2 µm filtered). The diluted plasma sample was centrifuged at 2000× *g* for 30 min (4 °C) to eliminate the cells and contaminating cell debris. The supernatant was further centrifuged at 10,000× *g* for 30 min at 4 °C to remove cellular debris and microvesicles. The supernatant was filtered using a 0.1 µm syringe filter (Millipore, Burlington, MA, USA) to further remove contaminating cell debris, microvesicles, and apoptotic bodies. The sample was ultracentrifuged at 100,000× *g* for 2 h at 4 °C (Optima L-100XP, 70.1 Ti rotor, Beckman Coulter, Sanford, FL, USA) to pellet the exosomes. Exosomes were then washed using 1× PBS (1 mL) to eliminate the contaminating proteins and pelleted again by UC at 100,000× *g* for 1 h at 4 °C. The final exosome pellet was re-suspended in 150 µL (50 µL/mL plasma) of 0.1 µm syringe-filtered 1× PBS for subsequent analysis.

The commercially available exoEasy Maxi kit (Qiagen GmbH, Hilden, Germany) was used according to the manufacturer's instructions with some modifications to the provided procedure. The plasma sample (3.4 mL) was diluted using filtered 1× PBS at 3:1 dilution and filtered using a 0.2 µm syringe filter (Millipore, Burlington, MA, USA). This was followed by adding XBP buffer (4.53 mL) to the diluted plasma (4.53 mL). The mixture was then added to the exoEasy spin column and centrifuged at 500× *g* for 1 min at 20 °C. The flow-through was discarded, and 10 mL of XWP buffer was added to the mixture, followed by centrifugation at 3000× *g* for 10 min at 20 °C to remove the residual buffer from the column. Then, the spin column was transferred to a new collection tube, and 800 µL of XE buffer was added to dissolve the exosomes. The spin column was then centrifuged at 500× *g* for 5 min at 20 °C to collect the eluate, which was added back to the spin column membrane and centrifuged at 3000× *g* for 10 min at 20 °C for another round of eluate collection. The purified exosomes were either used immediately or stored at −80 °C for further analysis.

2.3. Characterization of Exosomes

2.3.1. Particle Size, Concentration, and Surface Charge Analysis

Size distribution and particle concentration (particle number/mL) in exosome samples isolated by UC and kit method were determined by nanoparticle tracking analysis (NTA) using a NanoSight NS300 system (Malvern Technologies, Malvern, UK) configured with a 532 nm laser (green) and a high-sensitivity scientific CMOS (sCMOS) camera. Samples were prepared at an acceptable working concentration range (1×10^7 – 1×10^9 particles/mL) according to manufacturer's recommendations. Initially, 5 µL of purified exosome sample was diluted with 250 µL of 0.1 µm syringe-filtered 1× PBS (1:50 dilution). Sample was then diluted to 1:10, 1:20, and 1:100. These eventual 500×, 1000×, and 5000× diluted 1 mL samples were manually loaded into the chamber using 1 mL syringe. Among these, approximately 10–30 particles/frames showing sample was taken for further analysis. The

exosome movement and number of particles were recorded for 5×60 s (camera level = 15). A $0.1 \mu\text{m}$ syringe-filtered, particle-free $1 \times$ PBS (Gibco, Waltham, MA, USA) solution was used as a solvent. Capture settings (temperature, 22 ± 22.5 °C; slider shutter, 1300; slider gain, 295; number of frames, 1498) and analysis settings (detection threshold, 5; blur size, auto) were set, and particle movement data were analyzed using NTA 3.4 software. The zeta potential was measured using a zeta potential particle size analyzer (Zetasizer Nano ZSP, Malvern, UK). For NTA analysis, five repetitive measurements of an individual exosome sample from each UC and kit-based method were tested. For the zeta potential analysis, one individual exosome sample was tested from each method, and data were collected as average of triplicates.

2.3.2. Field-Emission Transmission Electron Microscopy (FE-TEM) Analysis

To verify the presence of exosomes and examine their morphology and size, FE-TEM analysis was performed based on methods described in a previous publication [21] with few modifications. Ten microlitres of each sample was placed onto formvar-carbon-coated copper grids for 10 min. The excess liquid was removed, and the grids were stained with 2.5% uranyl acetate for 1–2 s and air-dried for 5 min. The photographs were taken under an FE-TEM (model: Tecnai G2 F30 super-twin; FEI Company, Hillsboro, OR, USA) operating at an accelerating voltage of 300 keV.

2.3.3. Quantification of Intact and Lysed Exosome Protein Content

Intact exosome protein was quantified by Bradford assay following the manufacturer's protocol (Bio-Rad Laboratories, Inc., Hercules, CA, USA), and absorbance was measured at 595 nm. The exosome yield was determined based on the total protein content, which was calculated by multiplying the intact exosome protein concentration (mg/mL) by the volume of re-suspended exosomes [22]. Exosome recovery was calculated based on the total yield of protein per unit volume of plasma (protein mg/mL of plasma). In order to determine the total protein content, including luminal proteins, exosomes ($100 \mu\text{L}$) were mixed with $1 \times$ PBS ($100 \mu\text{L}$) and lysed by sonication (amplitude 30%, 10 s pulse repeated 3 times) using an ultrasonic processor (model: VCX 750, Sonics & Materials, Inc. Newtown, CT, USA), followed by protein quantification by Bradford assay.

2.3.4. Exosome Protein Profile Analysis by Coomassie and Silver Staining

To determine the protein profile of exosomes, sodium dodecyl sulphate-polyacrylamide gel electrophoresis (SDS-PAGE) was performed followed by Coomassie or silver staining with few modifications of methods described in previous studies [19,22]. Intact and sonicated exosome samples (without centrifugation) were separately diluted with $1 \times$ PBS to acquire equal amounts of proteins, mixed with $2 \times$ Laemmli sample buffer (Sigma-Aldrich, St. Louis, MO, USA) and then boiled at 95 °C for 5 min. Subsequently, two 12% SDS-PAGE gels were prepared and run in parallel with $25 \mu\text{g}$ of each sample loaded. One gel was subjected to staining with 0.05% Coomassie Brilliant Blue G-250 (Biosesang, Seongnam-si, Gyeonggi-do, Korea) followed by a standard de-staining procedure. The other gel was subjected to silver staining using the SilverQuest Silver Staining kit (Invitrogen, Life Technologies, Carlsbad, CA, USA).

2.3.5. Immunoblotting Analysis

To investigate the presence of exosome protein markers, immunoblotting analysis was performed using intact exosome samples. Subsequent to the determination of the protein concentration by means of the Bradford assay following the manufacturer's protocol, intact exosome samples isolated using both UC and the kit method were directly mixed with an equal volume of $2 \times$ Laemmli sample buffer. From each prepared sample, $16 \mu\text{g}$ of protein lysates were separated by 12% SDS-PAGE and blotted onto Immobilon-P polyvinylidene difluoride membranes (Millipore, Bedford, MA, USA). Membranes were blocked with 5% skim milk in TBS containing 0.05% Tween-20 and probed with primary antibodies overnight

at 4 °C. The antibodies used were CD63 rabbit pAb (#A5271; 1:1000; ABclonal, Woburn, MA, USA), Anti-CD81 (rabbit IgG) (#EXOAB-CD81A-1; 1:1000; System Biosciences), and HSP90 (#4874; 1:1000; Cell Signalling Technology, Danvers, MA, USA), all of which were polyclonal antibodies (pAb) produced against human proteins. After the membranes were washed three times with PBS containing 0.05% Tween20 (PBST) for 10 min, the membrane with CD81 primary antibody added to it was incubated for 1 h with goat anti-rabbit HRP secondary antibody (#EXOAB-HRP; 1: 20,000; System Biosciences, Palo Alto, CA, USA) diluted in 5% skim milk in TBST. The remaining membranes were incubated for 1 h with goat anti-rabbit IgG and HRP-conjugated antibody (#7074; 1:3000; Cell Signalling Technology, Danvers, MA, USA). All membranes were washed three times for 10 min with PBST. The signals of the HRP-conjugated antibodies were developed using Western blotting detection reagent (Western Femto ECL Kit, LPS Solution, Daejeon, Korea) and visualized using a chemiluminescence detection system (Fusion Solo S, Vilber, Lourmat, France).

2.4. *In Vitro* Cytotoxicity Assay

To determine the cytotoxicity of the rock bream exosomes isolated by UC and the kit method, the MTT (3-[4,5-dimethylthiazol-2-yl]-2,5-diphenyltetrazolium bromide) assay was performed in the FHM fish cells and RAW 264.7 mammalian cells. The FHM cell line was kindly gifted by Professor Sung-Ju Jung, Department of Aquatic Life Medicine, Chonnam National University, Yeosu, Korea. The RAW 264.7 cell line was provided by Professor Jong-Soo Lee, College of Veterinary Medicine, Chungnam National University, Daejeon, Korea. The FHM cell line was maintained at 20 °C in Leibovitz's L-15 (L-15) medium (Welgene, Gyeongsan-si, Gyeongsangbuk-do, Korea) supplemented with 10% foetal bovine serum (FBS) (Welgene, Gyeongsan-si, Gyeongsangbuk-do, Korea) and antibiotics (penicillin, 100 IU/mL; streptomycin, 100 µg/mL) (Gibco, NY, USA). The RAW 264.7 cells were maintained at 37 °C in a humidified atmosphere containing 5% CO₂ in Dulbecco's modified Eagle medium (Gyeongsan-si, Gyeongsangbuk-do, Korea) with 10% (*v/v*) FBS and antibiotic-antimycotic solution (Gibco™, Grand Island, NY, USA). For the assay, FHM cells were seeded into individual wells of a 96-well tissue culture microtitre plate (Becton, Dickinson and Co., Franklin Lakes, NJ, USA) at a cell density of 2 × 10⁵ cells/mL (0.1 mL) with 10% FBS containing L-15 media. After the plate was incubated at 20 °C for 24 h, the medium was replaced with fresh medium. RAW 264.7 cells were seeded at a density of 2 × 10⁵ cells/mL and allowed to adhere overnight, and the medium was replaced with fresh medium. The wells containing both cell types were treated in duplicates with different concentrations (6.25–100 µg/mL) of exosomes isolated by UC and the kit method. Here, the exosomes concentrations were based on the intact protein concentration of exosomes measured by the Bradford assay. Fresh culture medium was used as a negative control. PBS was used as the vehicle control for the ultra-centrifuged samples. For the kit-isolated exosome samples, the vehicle control comprised XE elution buffer diluted with nuclease-free water to obtain the same concentration and volume as that of each corresponding sample (Supplementary Figure S1). The plates were then incubated at the respective temperatures of FHM cells at 20 °C and RAW 264.7 cells at 37 °C for another 24 h, and the media was aspirated. From the 5 mg/mL of MTT (Sigma-Aldrich, St Louis, MO, USA) stock solution prepared in 1 × PBS, 10 µL was added to each well and incubated at 37 °C for 4 h. After removing the MTT, 50 µL of solubilization solution, dimethyl sulfoxide (Sigma-Aldrich, St Louis, MO, USA) was added and mixed to ensure complete solubilization of the formazan crystals. The absorbance was recorded at 595 nm using a microplate spectrophotometer (Bio-Rad Laboratories, Inc., Richmond, CA, USA).

2.5. *In Vitro* Immune Gene Transcriptional Analysis of Exosome-Treated FHM and RAW 264.7 Cells

To determine whether the exosomes derived from rock bream plasma isolated by UC had an immunomodulatory effect and/or any adverse immunogenic effect, mRNA expression analysis of selected immune functional genes was performed in exosome-

treated FHM and RAW 264.7 cells. The cells were maintained as per the aforementioned procedures. The FHM cells were seeded in a 24-well plate (5×10^5 cells/well) containing 0.5 mL of media and incubated overnight to facilitate cell attachment. RAW 264.7 cells at a concentration of 2.0×10^5 cells/mL were seeded in a 6-well plate (2 mL) and incubated overnight. The medium was replaced with exosome-depleted 5% FBS containing L-15 or DMEM, and the cells were treated with 25 and 50 $\mu\text{g}/\text{mL}$ of exosomes (three replicates per treatment). The normal cells without any treatment and the cells treated with $1 \times \text{PBS}$ were considered as the negative control and vehicle group, respectively. The cells were incubated at the respective temperatures (FHM cells at 20°C ; RAW 264.7 cells at 37°C), harvested at 24 h post-treatment (hpt), and snap-frozen in liquid nitrogen. RNA isolation was performed using the NucleoSpin RNA Mini kit (Macherey-Nagel, Duren, Germany) according to the manufacturer's protocol. Methods described in previously published studies were used to perform cDNA synthesis and reverse transcription quantitative real-time polymerase chain reaction (qRT-PCR) analyses [21]. The relative mRNA expression of each gene was calculated using the $2^{-\Delta\Delta\text{Ct}}$ method [23]. The mRNA expression of each gene in the FHM and RAW 264.7 cells was normalized to the housekeeping genes expressing β -actin and GAPDH, respectively. Fold change values were calculated by dividing the average relative gene expression level of each treated group by that of the vehicle group. Gene-specific primers and housekeeping genes for the two cell types are listed in Supplementary Table S1 [24–26].

2.6. Statistical Analysis

All analysis were conducted using GraphPad Prism software version 5 for Windows (GraphPad Software Inc., San Diego, CA, USA). The toxicity and gene expression data were analyzed statistically using one-way analysis of variance (ANOVA) followed by Tukey's multiple comparison test. Additionally, an unpaired two-tailed t-test was used to analyze the significant differences between the control and the treated (25 and 50 $\mu\text{g}/\text{mL}$) samples in terms of gene expression data and the in vitro toxicity data obtained for exosomes isolated by the kit-based method. Differences were considered significant at $p < 0.05$.

3. Results

3.1. Isolation and Characterization of Exosomes from Rock Bream

3.1.1. Determination of Exosome Yield and Recovery by Two Exosome Isolation Methods

Exosomes from the pooled plasma of healthy rock bream were isolated using two different exosome isolation methods: differential UC and the commercial exoEasy Maxi kit. Size distribution and concentration of particles, including protein concentrations of the exosomes isolated by the two methods, are summarized in Table 1. The total exosome yields of the two methods were determined by measuring the total protein content in the intact exosomes using the Bradford assay. The protein concentration of exosomes isolated by the UC method (2.65 mg/mL) was not significantly different ($p > 0.05$) compared to that of exosomes isolated by the kit method (2.33 mg/mL); however, the total yield was significantly ($p < 0.05$) higher for exosomes isolated by the kit method (1.86 mg ; $2.33 \text{ mg}/\text{mL} \times 0.8 \text{ mL}$) compared to that of exosomes isolated by the UC method (0.40 mg ; $2.65 \text{ mg}/\text{mL} \times 0.15 \text{ mL}$) (Table 1). Moreover, the recovery of the exosomes based on the protein by the kit method (0.55 mg/mL plasma) was higher compared to that of the UC method (0.12 mg/mL plasma) (Table 1).

Table 1. Particle distribution, size (mean and mode), particle concentration, zeta potential, total yield, and recovery of plasma derived from rock bream exosomes isolated by differential ultracentrifugation (UC) and exoEasy Maxi kit method.

Exosome Isolation Method	Size Range (nm)	Mean Size (nm)	Mode Size (nm)	Zeta Potential (mv)	Particle Con. (particles/mL)	Protein Con. (mg/mL)	Total Yield (mg)	Protein Recovery (mg/mL plasma)
UC	D10: 65.7 ± 2.8 D50: 97.4 ± 5.0 D90: 176.5 ± 7.3	114.6 ± 4.6	83.1 ± 7.7	−19.90 ± 3.47 ^a	$4.90 \times 10^{10} \pm 2.91 \times 10^9$ ^a	2.65 ± 0.01 ^a	0.40 ± 0.0 ^a	0.12 ± 0.0 ^a
exoEasy Maxi kit	D10: 62.5 ± 1.3 D50: 90.8 ± 3.3 D90: 195.2 ± 5.7	111.2 ± 2.2	68.4 ± 2.7	−27.00 ± 3.57 ^b	$1.05 \times 10^{11} \pm 1.23 \times 10^{10}$ ^b	2.33 ± 0.03 ^b	1.86 ± 0.03 ^b	0.55 ± 0.01 ^b

Particle size distribution and particle concentration data represent the average of five repetitive measurements from an individual exosome sample of each UC and kit-based method. Zeta potential, protein concentration, total yield, and the protein recovery data represent the average of triplicate measurements from an individual exosome sample of each UC and kit-based method. Data are presented as mean ± standard error (SE). Values of each parameter tested for the exosomes isolated by UC and kit-based methods were statistically analyzed by unpaired two-tailed *t*-test, and significant differences are shown by different letters. Statistical significance was set as $p < 0.05$.

3.1.2. FE-TEM Analysis

FE-TEM analysis was used to characterize the morphology and size of the exosomes isolated by UC and the kit-based method. In the samples isolated by UC, the small membrane vesicles had diameters approximately in the range of 50–175 nm and cup-shaped structures that are typical of exosomes (Figure 1(A-1,A-1')). Samples isolated by the kit-based method showed intact exosomes with comparatively clearer margins and typical cup-shaped structures; however, more size heterogeneity (29–195 nm) was observed among these exosomes (Figure 1(B-1,B-1')). The “cup-shape” is a commonly applied morphological definition in analysis of Evs for samples observed using TEM [27]. The Evs generally appear as “cup shaped” because of dehydration during sample preparation [28].

3.1.3. Size Distribution, Particle Size, Zeta Potential, and Particle Concentration Obtained from Two Exosome Isolation Methods

The particle diameter and concentration of the exosomes were determined by NTA, which showed the exosome particle diameter to be in the range of 60–200 nm (Table 1). For the ultracentrifuged exosomes, the mean size, mode size, and concentration were 114.6 ± 4.6 nm, 83.1 ± 7.7 nm, and $4.90 \times 10^{10} \pm 2.91 \times 10^9$ particles/mL, respectively, whereas the same measurements for exosomes isolated by the kit were 111.2 ± 2.2 nm, 68.4 ± 2.7 nm, and $1.05 \times 10^{11} \pm 1.23 \times 10^{10}$ particles/mL, respectively. The particle diameter size ranges of exosomes isolated by UC (D10, 65.7 ± 2.8; D50, 97.4 ± 5.0; and D90, 176.5 ± 7.3), and the kit method (D10, 62.5 ± 1.3, D50, 90.8 ± 3.3; and D90, 195.2 ± 5.7) showed similar D10 and D50 values for both methods. However, the D90 value varied between the two methods to some extent, indicating that the 90% of the particle sizes were below 176.5 ± 7.3 and 195.2 ± 5.7 for exosomes isolated by UC and the kit method, respectively.

3.1.4. Protein Profiling and Immunoblotting Analysis of Exosomes Isolated by the Two Methods

SDS-PAGE of samples subjected to Coomassie and silver staining (Figure 2A,B) demonstrated that intact or sonicated exosome protein profiles did not change markedly for exosomes isolated by the two methods. However, more comparatively prominent protein bands were observed in the lysates of the exosomes isolated by UC (sizes: 25–35 kDa, P4, P5, and P6; 63–75 kDa, P7 and P8; and 100–135 kDa, P9 and P10) and in the crude plasma than those in the exosomes isolated by the kit method (Figure 2A,B). Moreover, there were some bands which did not appear in the lysates of exosomes isolated by UC but can be seen in the lysates of exosomes isolated by the kit-based method (sizes: 11–20 kDa, P11, P12, P13, and P14; 20–25 kDa, P15 and P16; 75–100 kDa, P17) (Figure 2A,B). We identified some of

the proteins based on their size range; for example, P1, P2, and P3 were identified as CD81, CD63, and Hsp90, respectively. However, it was difficult to accurately determine the exact identity of the proteins appearing in the SDS-PAGE protein profile without performing protein analysis using mass spectrometry.

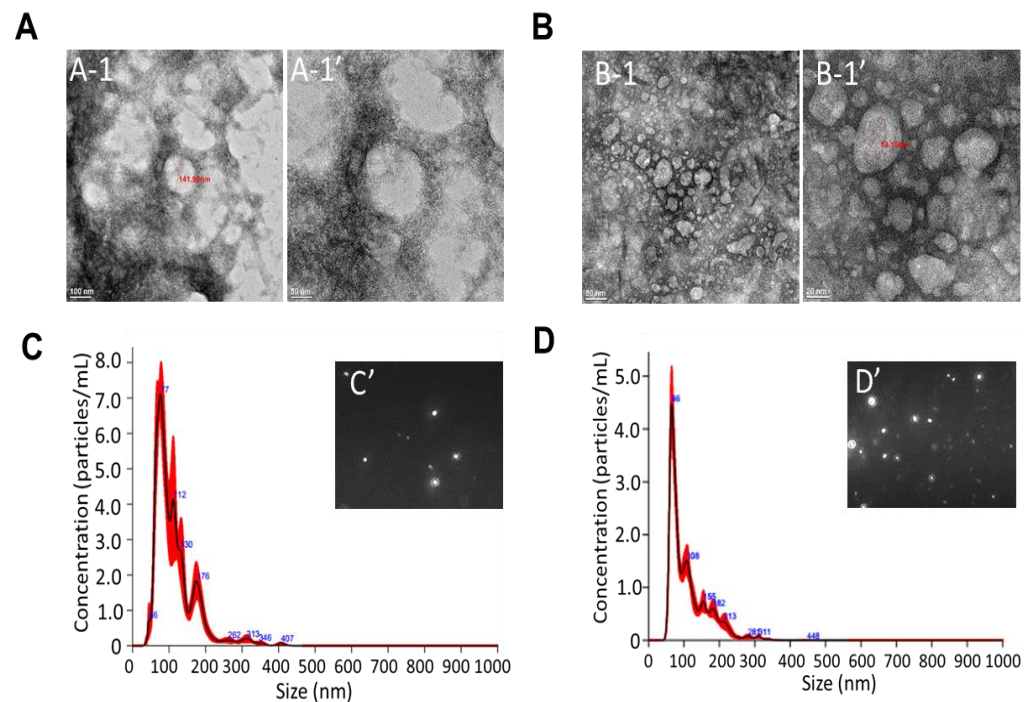


Figure 1. Isolation and characterization of exosomes derived from rock bream plasma by differential ultracentrifugation (UC) and using exoEasy Maxi kit (kit). Representative electron microscopy images of (A) ultracentrifuged and (B) exoEasy Maxi kit-derived exosomes (scale bar for (A-1); 100, (A-1') 50, (B-1); 50 (B-1'); and 20 nm). The nanoparticle tracking analysis (NTA) representing size distribution and concentration profile of the plasma-derived exosomes isolated by (C) UC and (D) exoEasy Maxi kit. The line graphs are based on the average of five repeated measurements of one individual sample. Particle images of ultracentrifuged and exoEasy Maxi kit-derived exosomes taken during NTA analysis are represented as (C') and (D'), respectively. Size distribution and concentration of particles including Bradford protein concentrations of isolated exosomes by two methods are summarized in Table 1.

To further analyze the efficacy of the isolation methods and to confirm the existence of exosomes, we used immunoblotting to investigate the presence of certain ubiquitous exosome marker proteins, namely, two tetraspanins (CD63 and CD81) and exosome-enriched heat shock protein Hsp90. We observed CD81 to be present in higher amounts in exosomes isolated by the kit method than in those isolated by UC. CD63 and Hsp90 were found in the exosomes isolated by both methods (Figure 2C). Moreover, CD63 and Hsp90 were prominently observed in the plasma lysate, whereas CD81 had a negligible presence. As expected, the data indicate the successful isolation and presence of exosomes in the samples; however, the levels of purity seemed to vary for different procedures of exosome isolation.

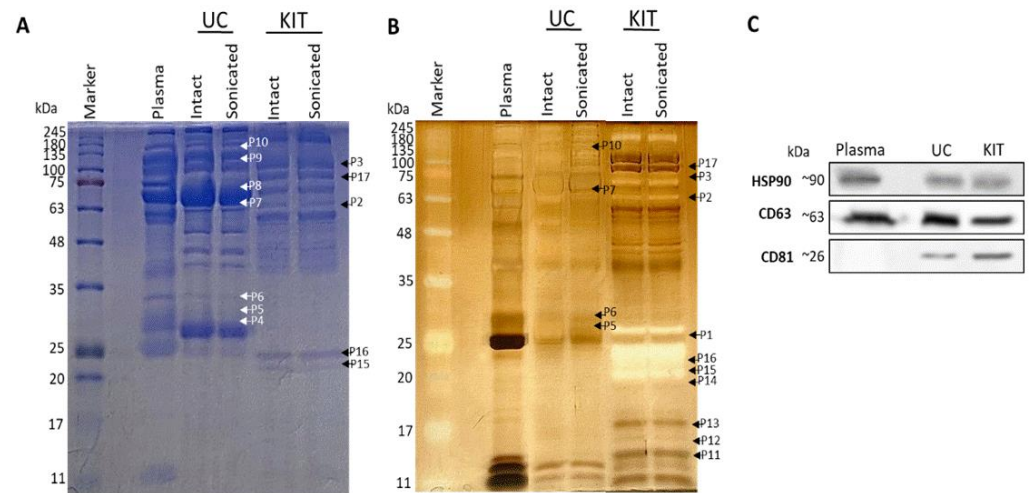


Figure 2. Total protein profile and immunoblotting analysis of exosome markers of rock bream plasma-derived exosomes by differential ultracentrifugation (UC) and exoEasy Maxi kit. Proteins (25 µg protein per lane) of ultracentrifuged and kit-isolated exosomes were separated by SDS-PAGE to represent the protein profile after (A) Coomassie and (B) silver staining. Proteins labelled based on the size range (P1–P17) obtained by SDS-PAGE. (C) Proteins (16 µg protein per lane) were separated by SDS-PAGE and immunoblotted with antibodies against CD81, CD63, and Hsp90.

3.2. In Vitro Cytotoxicity Analysis

In vitro cytotoxicity was tested for the exosomes isolated from FHM and RAW 264.7 cells by both methods (UC and kit-based method). The exosome concentration range used for the treatments was 6.25–100 µg/mL. The results show no significant enhancement of cell death or cytotoxicity (>80% cell viability) upon treatment with exosomes isolated by UC (Figure 3A,B) compared to that observed for treatment with the control or the vehicle. In contrast, significant ($p < 0.05$) cytotoxicity (<80% cell viability at >12.5 µg/mL) to both cell types was observed upon treatment with exosomes isolated by the kit (IC₅₀: FHM cells, 10.13 µg/mL; RAW 264.7 cells, 42.68 µg/mL) and solely by the XE elution buffer (IC₅₀: FHM cells, 7.84 µg/mL; RAW 264.7 cells, 32.86 µg/mL) compared to that observed by treatment with the control (Supplementary Figure S1). Based on these cytotoxicity data, exosomes isolated using the UC method were selected for further experiments.

3.3. In Vitro Immune Gene Transcriptional Analysis upon Exosome Treatment

In order to determine the immunomodulatory and/or adverse immune gene responses elicited in the cells upon treatment with naive rock bream exosomes (25 and 50 µg/mL), mRNA expression of several immune functional genes was analyzed *in vitro*. In FHM cells, the seven genes tested were those related to the chemokine (IL8), transcription factor (NF-κB), tumour-suppressor protein (p53), anti-viral (IRF7, IFN, and Mx1), and the stress response protein (HspB8). In RAW 264.7 cells, a total of ten genes were analyzed, which were related to Toll-like receptors (Tlr2 and Tlr4, pro-inflammatory cytokines (Il6 and Tnfα), the chemokine (Il-1β), the antimicrobial enzyme (Lyz1), antiviral Ifnβ1, Isg20, and Mx1), and the anti-oxidant (Sod1). Figure 4 shows the relative mRNA expression fold change values of immune-related genes in FHM (Figure 4A) and RAW 264.7 cells (Figure 4B) for 25 and 50 µg/mL exosome treatment compared to those for the vehicle treatment at 24 hpt. The FHM cells showed a slightly higher or basal level mRNA expression for p53 (1.14-fold), Ifn (1.01-fold), and Mx1 (1.16-fold) genes with 25 µg/mL exosome treatment compared to those observed for treatment with the vehicle control. A dose-dependent increase was observed in the mRNA expression levels of Il8 (25 µg/mL, 0.75-fold and 50 µg/mL, 0.85-fold) and Irf7 (25 µg/mL, 0.78-fold and 50 µg/mL, 0.82-fold); however, these values were lower and not significantly different from those obtained by the vehicle treatment (1-fold). Moreover, a dose-dependent decrease was observed in the levels of NF-

κ B (25 μ g/mL, 0.87-fold and 50 μ g/mL, 0.72-fold), p53 (25 μ g/mL, 1.14-fold and 50 μ g/mL, 0.88-fold), Ifn (25 μ g/mL, 1.01-fold and 50 μ g/mL, 0.70-fold), Mx1 (25 μ g/mL, 1.16-fold and 50 μ g/mL, 0.92-fold), and Hsp8B (25 μ g/mL, 0.87-fold and 50 μ g/mL, 0.69-fold). Except for NF- κ B mRNA expression at 50 μ g/mL ($p < 0.05$), these changes were not statistically significant compared to those observed for vehicle treatment. The gene expression fold change for 25 and/or 50 μ g/mL exosome treatment did not exceed 1.16-fold and did not decrease below 0.69-fold for the FHM cells at 24 hpt.

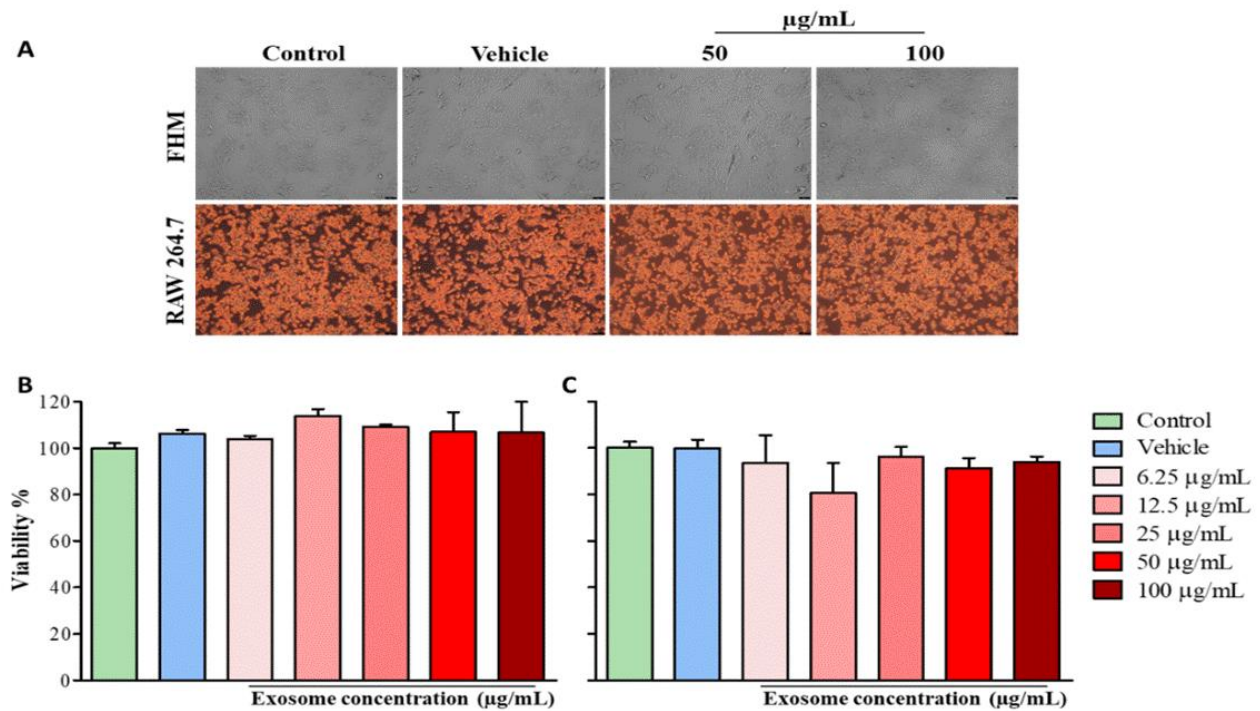


Figure 3. Cytotoxicity of the rock bream plasma-derived exosomes isolated by UC from fish and mammalian cells. Representative images illustrate the (A) cell morphology of fathead minnow (FHM) and RAW 264.7 cells observed under an inverted light microscope (Leica DMi8, Germany) with different exposure conditions (control, vehicle, and 50 and 100 μ g/mL exosome treatment). Scale bar, 200 μ m. Graphs depicted the cell viability of exosomes at different concentrations (6.25–100 μ g/mL) for (B) FHM and (C) RAW 264.7 cells. A total of 1 mg/mL of exosome stock solution was used to prepare the samples with the respective final concentrations. Data are presented as mean \pm standard error (SE). One-way ANOVA was performed to test statistical significance. Statistical significance was set as $p < 0.05$.

In RAW 264.7 cells, mRNA expression levels of most of the tested genes (Tlr2, Tnfa, Il1 β , Lyz1, Ifn β 1, Isg20, and Mx1) were slightly higher (≥ 1.2 -fold) or at the basal level for 25 and/or 50 μ g/mL exosome treatment compared to those of the vehicle control group. Among these, Lyz1 expression showed a significant difference ($p < 0.05$) between the vehicle control group and 50 μ g/mL exosome treatment group. The mRNA expression levels of Tlr4 (0.74-fold), Il6 (0.74-fold), and Sod1 (0.90-fold) in 25 μ g/mL treated cells were lower than those in the vehicle control group, but the values were not significantly different. The highest gene expression, either at 25 and/or 50 μ g/mL, did not exceed 1.53-fold and was not lower than 0.74 in the RAW 264.7 cells at 24 hpt.

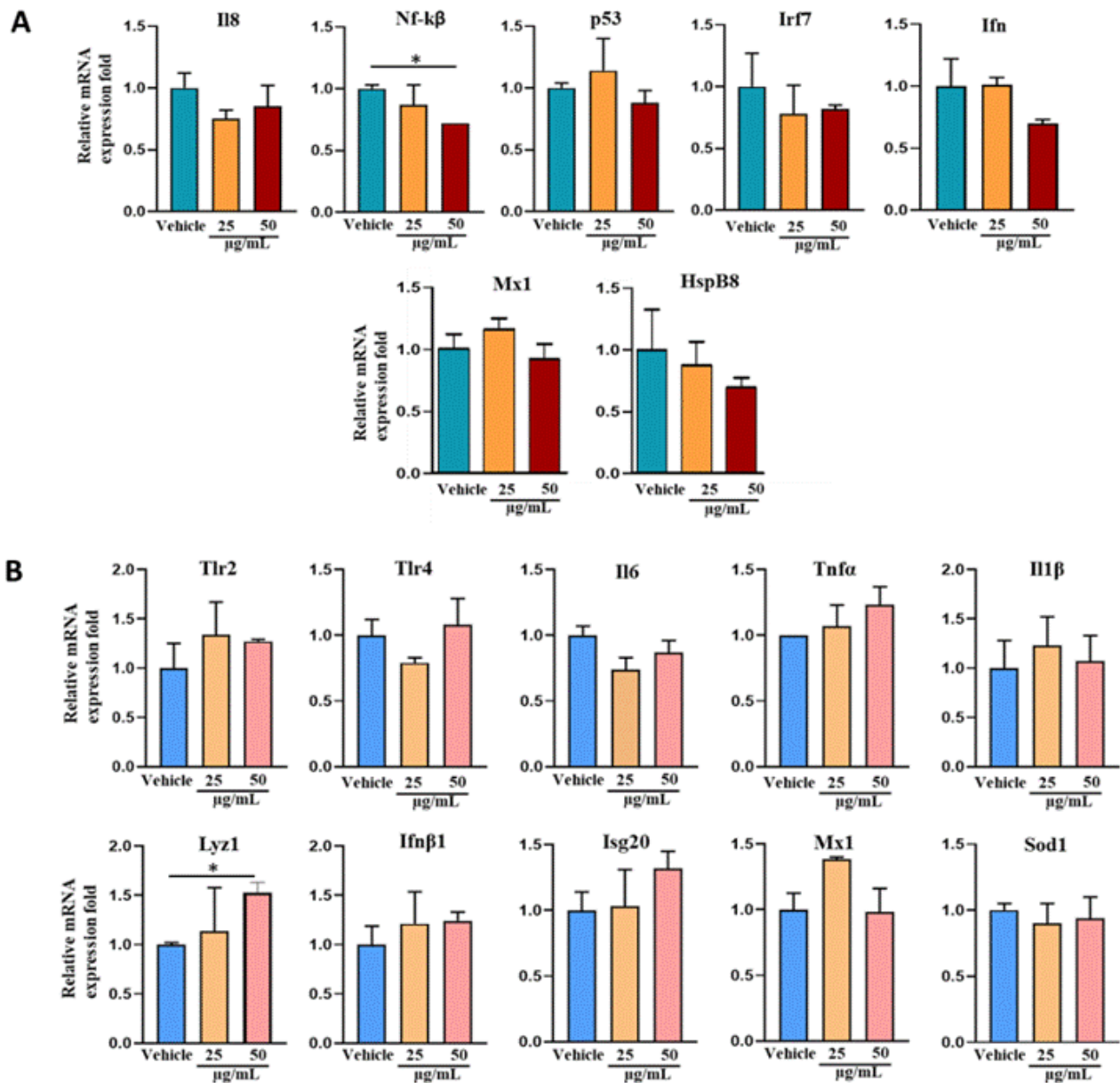


Figure 4. *In vitro* immune gene expression analysis of cells at 24 hpt treated with rock bream plasma-derived exosomes isolated by ultracentrifugation (UC). mRNA expression was analyzed in (A). Fathead minnow (FHM) cells and (B). RAW 264.7 cells with different exposure conditions (vehicle, 25, and 50 µg/mL exosome treatment). Data are presented as mean ± standard error (SE). Unpaired two-tailed *t*-test was used to analyze the significant differences between the control and the treated (25 and 50 µg/mL) samples. Statistical significance was set at $p < 0.05$. Asterisk (*) indicates a significant difference in expression levels compared to those of the vehicle control.

4. Discussion

Exosomes serve as potential drug delivery vehicles owing to their inherent characteristics, such as low immunogenicity, stability, target delivery, and ability to pass natural barriers, and can thus be used for treating various diseases [29,30]. In this study, exosomes from rock bream plasma were isolated using the current gold-standard procedure, UC, and the spin column-based exoEasy Maxi kit, and basic physicochemical and morphological characteristics of exosomes obtained by the two methods were compared for the first time. To the best of our knowledge, exosomes in rock bream fish have not been characterized in depth. Our TEM results indicated that exosomes isolated by both methods have sizes in

the range of 20–200 nm and were cup-shaped, membrane-bound vesicles similar to those described in previously published studies [5,13,31]. The purity of the isolated exosomes was verified in terms of the absence of apoptotic bodies or cell debris. Both methods yielded heterogeneous exosomes. Exosomes isolated by the kit-based method were observed to be intact membrane-bound vesicles with less granular background staining compared to those obtained by the UC method. This observation suggests UC-based exosome isolation includes the presence of other particles (soluble proteins, low-density lipoproteins, etc.) that precipitate together with the exosomes, which does not occur with the membrane affinity kit-based method due to its highly selective nature for EV isolation [32], resulting in fewer impurities during isolation. Previous studies reported the use of TEM to confirm the isolation of differentially ultracentrifuged trout plasma-derived exosomes with an average diameter of 54 ± 4 nm [7] and exosomes derived from the serum of male and female *Cynoglossus semilaevis* fish as being spherical and having a diameter in the range of 30–120 nm [8]. Garcia et al. presented TEM results showing EV-like structures isolated from culture supernatants by differential UC, and the samples isolated by the exoEasy Maxi kit had sizes ranging between 30 and 300 nm and 100 and 200 nm, respectively [33]. Moreover, in these studies, the authors reported cup-shaped EV-like structures in TEM images of exosomes isolated from human plasma by differential UC; however, amorphous materials derived from plasma constituents, such as proteins and lipids, were reported to be co-isolated with these EV-like structures. Furthermore, they stated that EV-like structures could not be observed in the samples isolated using the exoEasy Maxi kit due to the presence of amorphous materials and possibly the low abundance of EVs. In light of these facts, our TEM results indicate that rock bream plasma-derived exosomes are distinctly a heterogeneous population of vesicles, and the modifications made to the original procedure of exosome isolation using the exoEasy Maxi kit may enhance the efficiency of the isolation procedure in terms of purity to some extent.

NTA analysis was performed to quantitatively measure the size distribution and particle concentration of the exosomes. Exosomes obtained by both isolation methods had a similar average diameter (exosome mean size: UC, 114.6 ± 4.6 ; kit, 111.2 ± 2.2 nm) within the expected range [30]. The most predominant particle sizes detected varied between the two methods (exosome mode size: UC, 83 nm; kit, 68.4 nm). However, 90% of the exosome population in the UC sample and the kit sample had particle sizes below 176.5 nm and 195.2 nm, respectively. In this study, the kit method yielded exosomes with a higher average size in comparison to that of those obtained by UC, which was consistent with the results of a previous study [33]. Another study reported the isolation of serum-derived EVs from *Piscirickettsia salmonis*-infected and non-infected Atlantic salmon (*Salmo salar*) using the same commercial kit, which had a high average particle diameter ranging between 230 and 300 nm [9]. Vesicle sizes obtained by UC (173 nm) have been reported to be comparatively similar but slightly higher than those obtained by the recently developed membrane affinity column-based method (160 nm) [32]. In accordance with these results, in this study, we observed a slightly higher average particle diameter for exosomes isolated by the UC method (114 nm) than for those isolated by the kit-based method (111 nm). This suggests that both methods could successfully purify the exosome fractions separating out the large protein particles in the centrifugation supernatant or the column flow-through during UC and the kit process, respectively. However, the particle concentration was 10-fold higher for the kit-based method than that obtained by UC, and this result is consistent with previous reports [32,33]. The UC technique uses a high centrifugal force ($100,000 \times g$), which might result in breakage of some of the EV particles. It has been reported that particles smaller than 60 nm cannot be detected by NS300; thus, broken particles may be undetectable [33]. Hence, exosomes isolated by the exoEasy Maxi kit might have more intact particles, thereby giving this method a higher particle count. The zeta potential is an important factor for evaluating the dispersion stability and integrity of freshly isolated exosomes [30]. High dispersion stability is indicated by the higher negative magnitude of the zeta potential. A high dispersion stability is indicated by the higher negative magnitude of the zeta

potential. It has been reported that very low negative surface charges of exosomes can disturb dispersion stability and biological functionality. In this study, exosomes isolated by the kit-based method showed a comparatively higher surface negative charge (-27 mV) compared to that of those isolated by UC (-19.9 mV), suggesting higher repulsion between the particles in a suspension with high dispersion stability. However, considering the negative magnitude values reported in previous studies, we postulate that exosomes isolated by UC also have an acceptable level of dispersion stability [30].

To verify the existence of exosomes, the levels of known exosome-enriched protein markers, the tetraspanins CD81 and CD63 and the heat shock protein Hsp90, were determined in the isolated exosome samples by immunoblotting [8,12,34]. Comparable levels of these marker proteins were detected in the exosome samples isolated by both UC and the kit-based method. However, the detection levels varied between the two isolation methods, which is consistent with results reported in previous studies [33]. Moreover, in this study, bands corresponding to CD63 and Hsp90 were found to be abundant in the crude plasma lysate. We postulate that the presence of EVs in the crude plasma may be the reason for this observation. However, due to the lack of studies reporting similar gel-based results, this claim cannot be established conclusively. Although immunoblotting is a widely used technique for protein marker detection, non-specific binding, and contamination during the detection of exosome marker proteins is a common issue in the field of exosome research and results in false interpretations. Physiological diversity, artefactual chemical modifications, and post-translational modifications are known to result in extra bands or observable bands that are different from the expected size [35]. Moreover, nonspecific antibody binding is a common issue associated with extra bands. In this study, we used rabbit polyclonal antibodies, which are produced against human proteins, due to the unavailability of the teleost-specific antibodies. The difference in the homology of these molecules between teleost and mammalian counterparts might have resulted in the possibility of primary antibodies having affinity towards other proteins as well. Therefore, as supportive evidence for our results, full blots are provided (Supplementary Figure S2). Moreover, due to the insufficient availability of annotated sequence databases for most teleosts, it is difficult to determine whether fish cell subsets express the same molecules (e.g., CDs) as their mammalian counterparts. Thus, choosing suitable primary antibodies for these molecules is crucial for minimizing cross-reactivity or nonspecific binding, thereby avoiding false interpretation. Therefore, we suggest that during the characterization of exosomes from teleosts, Western blotting may be inadequate in terms of avoiding false interpretations by minimizing cross-reactivity and nonspecific binding. Hence, in future studies, mass spectrometry-based proteomics profile analysis should be considered as an apt method for confirmation of exosome-enriched protein markers in teleosts such as rock bream fish.

The advantages and disadvantages of different exosome isolation methods and their applications in different types of research have been reported [30,32]. The combination of other polymer-based precipitation techniques with several rounds of UC is considered more suitable for eliminating impurities, although the yield is reported to decrease to some extent [36]. Among the protein bands displayed in the stained SDS-PAGE gels, some of the proteins in the plasma lysate were overrepresented in the UC-derived exosome lysate compared to those in the exosome lysate of the kit-based method. Moreover, we observed that exosomes isolated by UC had higher protein concentrations than those of the exosomes isolated by the kit-based method and possibly incorporate some contaminant proteins during the process. Even though it is challenging to separate plasma exosomes from plasma proteins and other contaminants, we postulate that most of the abundant larger protein complexes present in the plasma can be removed during the binding and washing steps for the kit-based method, thereby obtaining comparatively high purity exosomes. Considering our results along with evidence from previous studies, we recommend that it is important to choose a particular optimized isolation method to maintain consistency because different isolation methods may result in discrepancies in size, particle concentration, and purity of

the exosomes, which may affect downstream applications, such as biological functional analysis, mRNA, miRNA, and proteomic analysis [30,32–34].

Previous studies on the immunomodulatory functions of exosomes derived from immune-activated murine macrophage cells [37] and the presence of antigenic viral proteins in porcine serum-derived exosomes [38] suggest the future prospects of using exosomes as carriers of therapeutic molecules for inflammatory pain and as candidates for vaccine delivery, respectively. The involvement of exosomal miRNAs in the antiviral immune response in aquatic invertebrates (crustaceans) and evidence for the antiviral role of exosomes in teleosts have also been reported [10,11,13]. Furthermore, secretion of exosomes from antigen-presenting cells with an abundance of immune molecules such as MHCII β upon treatment with chemical stimulants such as CpG and differential protein expression patterns in the EVs of *S. salar* that are released from the infected cells to promote immune responses upon treatment with biological stimulants, such as *P. salmonis*, has been reported [6,9]. Based on the above facts, we postulate that rock bream plasma exosomes may also be used as carriers for therapeutic agents or antigen proteins, and thus, they may be used for the production of therapeutic exosomes for fish medicine. However, before testing the biological effects of exosomes *in vivo*, it is important to carry out toxicity and immunogenicity studies, especially when developing exosome-based therapeutic targets [39]. In this study, although the kit-based procedure resulted in a better exosome yield, required less time for isolation, and was easily adapted to laboratory workflows compared to the UC method, it showed one limitation during *in vitro* toxicity studies, which was the toxicity of the XE elution buffer. This prompted us to utilize the UC procedure for further functional analysis studies, unless additional steps provided in the exoEasy Maxi Kit Handbook in Appendix C on page 22 were to be followed for the elimination of cytotoxicity. However, considering that no toxicity (>80% cell viability) was observed in FHM and RAW 264.7 cells when treated with exosomes isolated by UC, thus suggesting the safety of these exosomes, we proceeded with further experiments using exosomes isolated by UC to analyze the immunomodulatory effects or occurrence of adverse immune responses due to naïve exosome treatment. The mRNA expression levels of the tested antiviral (Irf7, Ifn, and Mx₁), tumour suppressor protein (p53), chemokines (Il8), and the heat shock protein (Hsp8B) genes were not significantly altered compared to those of the control at 24 hpt in FHM cells, suggesting no apparent adverse responses occurred. Moreover, except the slightly, but significantly ($p < 0.05$) induced bacterial defence enzyme Lyz1 gene, the pattern recognition receptors Tlr2 and Tlr4, inflammatory factors Il6, Tnf α , and Il1 β , antiviral genes Ifn β 1, Mx1, and Isg20, and the antioxidant gene Sod1 in RAW 264.7 cells had either basal or slightly induced expression in a dose-dependent manner. These data confirm the absence of significant immunomodulatory effect or any apparent adverse immune induction or suppression with no cytotoxicity being observed upon treatment with naïve rock bream exosomes; however, further time point analysis, different dose trials, and testing more genes will be required for further validation. It has been reported that engineered exosomes have a function of immune regulation and coordinating innate and adaptive immune reactions and thereby have great potential in various biomedical applications [3]. We postulate that the exosomes isolated from rock bream could be used as carriers of therapeutic molecules for various biological applications in fish medicine, such as wound-healing, anti-inflammatory antimicrobial action, and the development of vaccines, when incorporated with specific miRNAs, peptides, antigens, or other drugs. However, future functional studies are required to analyze exosomes in terms of safety and improve the efficiency of exosome-based treatments.

5. Conclusions

In this study, for the first time we demonstrated the existence of exosomes in the plasma of rock bream. Morphological and physicochemical characterization results indicate that we successfully isolated exosomes from rock bream plasma, which were observed to have sizes (mean diameter of UC and kit: 114.6 ± 4.6 and 111.2 ± 2.2 nm, respectively) within the

reported exosome size range. Moreover, we report that the commercially available exoEasy membrane affinity kit used for the isolation of exosomes from rock bream blood plasma yields higher particle concentration and recovery and has fewer contaminants compared to UC isolation. However, exosomes isolated by UC did not induce cytotoxicity *in vitro*, indicating that they can be used directly for downstream biological response analysis, whereas exosomes isolated by the kit-based method require certain buffer exchange steps to be additionally performed as recommended by the manufacturer to eliminate cytotoxic effects. In the future, RBIV-infected rock bream plasma exosomes characterization at the molecular (proteomics and miRNAs) level may provide reliable informative facts as they may be similar to or different from their parent cells. As active intercellular communicators, such exosomes may offer prospective diagnostic and therapeutic value in pathogen identification in aquaculture.

Supplementary Materials: The following supporting information can be downloaded at: <https://www.mdpi.com/article/10.3390/fishes7010036/s1>. Figure S1: Cytotoxicity of the plasma-derived exosomes of rock bream isolated by exoEasy Maxi kit on the fathead minnow (FHM) fish cells and RAW 264.7 mammalian cells. Figure S2: Full gel blots correspond to immunoblotting analysis of exosome markers of rock bream plasma-derived exosomes by differential ultracentrifugation (UC) and exoEasy Maxi kit. Table S1: Primers used in this study.

Author Contributions: Conceptualization, C.N. and M.D.Z.; Formal analysis, C.N., E.H.T.T.J., S.L.E., D.C.R., W.P.W., and J.N.C.J.; Funding acquisition, C.N.; Investigation, C.N., E.H.T.T.J., W.P.W. and J.N.C.J.; Methodology, C.N., E.H.T.T.J., S.L.E., and M.D.Z.; Project administration, C.N. and M.D.Z.; Resources, M.D.Z.; Supervision, C.N. and M.D.Z.; Writing—original draft, C.N.; Writing—review and editing, C.N., E.H.T.T.J., S.L.E., D.C.R., W.P.W., J.N.C.J., and M.D.Z. All authors have read and agreed to the published version of the manuscript.

Funding: This work was supported by the National Research Foundation of Korea (NRF) grants, funded by the Korea government (MSIT) 2021R1A2C1004431).

Institutional Review Board Statement: All experiments with rock bream fish were conducted in accordance with the approved guidelines and regulations of the Animal Ethics Committee of Chungnam National University (202103A-CNU-105).

Data Availability Statement: The data presented in this study are available on request from the corresponding author.

Conflicts of Interest: The authors declare no conflict of interest.

References

1. Gurung, S.; Perocheau, D.; Touramanidou, L.; Baruteau, J. The exosome journey: From biogenesis to uptake and intracellular signaling. *Cell Commun. Signal.* **2021**, *19*, 47. [[CrossRef](#)] [[PubMed](#)]
2. Li, X.; Corbett, A.L.; Taatizadeh, E.; Tasnim, N.; Little, J.P.; Carnis, C.; Daugaard, M.; Guns, E.; Hoorfar, M.; Li, I.T.S. Challenges and opportunities in exosome research—perspectives from biology, engineering, and cancer therapy. *APL Bioeng.* **2019**, *3*, 011503. [[CrossRef](#)] [[PubMed](#)]
3. Kalluri, R.; LeBleu, V.S. The biology, function, and biomedical applications of exosomes. *Research* **2020**, *367*, eaau6977. [[CrossRef](#)] [[PubMed](#)]
4. Gomez, C.D.L.T.; Goreham, R.V.; Serra, J.J.B.; Nann, T.; Kussmann, M. “Exosomics”—A review of biophysics, biology, and biochemistry of exosomes with a focus on human breast milk. *Front. Genet.* **2018**, *9*, 92. [[CrossRef](#)]
5. Schorey, J.S.; Cheng, Y.; Singh, P.P.; Smith, V.L. Exosomes and other extracellular vesicles in host-pathogen interactions. *Rev. EMBO Rep.* **2015**, *16*, 24–43. [[CrossRef](#)]
6. Iliiev, D.B.; Jorgensen, S.M.; Rode, M.; Krasnov, A.; Harneshaug, I.; Jorgensen, J.B. CpG-induced secretion of MHCII β and exosomes from salmon (*Salmo salar*) APCs. *Dev. Comp. Immunol.* **2010**, *34*, 29–41. [[CrossRef](#)]
7. Faught, E.; Henriskson, L.; Vijayan, M.M. Plasma exosomes are enriched in Hsp70 and modulated by stress and cortisol in rainbow trout. *J. Endocrinol.* **2017**, *232*, 237–246. [[CrossRef](#)]
8. Sun, Z.; Hao, T.; Tian, J. Identification of exosomes and its signature miRNAs of male and female *Cynoglossus semilaevis*. *Sci. Rep.* **2017**, *7*, 860. [[CrossRef](#)]
9. Lagos, L.; Tandberg, J.; Kashulin-Bekkelund, A.K.; Colquhoun, D.J.; Sorum, H.; Winther-Larsen, H.C. Isolation and characterization of serum extracellular vesicles (EVs) from Atlantic salmon infected with *Piscirickettsia Salmonis*. *Proteomes* **2017**, *5*, 34. [[CrossRef](#)]

10. Yang, H.; Li, X.; Ji, J.; Yuan, C.; Gao, X.; Zhang, Y.; Lu, C.; Li, F.; Zhang, X. Changes of microRNAs expression profiles from red swamp crayfish (*Procambarus clarkia*) hemolymph exosomes in response to WSSV infection. *Fish. Shellfish Immunol.* **2019**, *84*, 169–177. [[CrossRef](#)]
11. Gong, Y.; Kong, T.; Ren, X.; Chen, J.; Lin, S.; Zhang, Y.; Li, S. Exosome-mediated apoptosis pathway during WSSV infection in crustacean mud crab. *PLoS Pathog.* **2020**, *16*, e1008366. [[CrossRef](#)] [[PubMed](#)]
12. Zhao, N.; Zhang, B.; Xu, Z.; Jia, L.; Li, M.; He, X.; Bao, B. Detecting *Cynoglossus semilaevis* infected with *Vibrio harveyi* using micro RNAs from mucous exosomes. *Mol. Immunol.* **2020**, *128*, 268–276. [[CrossRef](#)] [[PubMed](#)]
13. He, J.; Chen, N.N.; Li, Z.M.; Wang, Y.Y.; Weng, S.P.; Guo, C.J.; He, J.G. Evidence for a novel antiviral mechanism of teleost fish: Serum-derived exosomes inhibit virus replication through Incorporating Mx1 protein. *Int. J. Mol. Sci.* **2021**, *22*, 10346. [[CrossRef](#)] [[PubMed](#)]
14. Jung, S.J.; Oh, M.J. Iridovirus-like infection associated with high mortalities of striped beakperch, *Oplegnathus fasciatus* (Temminck et Schlegel), in southern coastal areas of the Korean peninsula. *J. Fish. Dis.* **2000**, *23*, 223–226. [[CrossRef](#)]
15. Kurita, J.; Nakajima, K. Megalocytiviruses. *Viruses* **2012**, *4*, 521–538. [[CrossRef](#)]
16. Jung, M.H.; Chico, V.; Ciordia, S.; Mena, M.C.; Jung, S.J.; Villaizan, M.D.M.O. The Megalocytivirus RBIV induces apoptosis and MHC Class I presentation in rock bream (*Oplegnathus fasciatus*) red blood cells. *Front. Immunol.* **2019**, *10*, 160. [[CrossRef](#)]
17. Chico, V.; Puente-Marin, S.; Nombela, I.; Ciordia, S.; Mena, M.C.; Carracedo, B.; Villena, A.; Mercado, L.; Coll, J.; Ortega-Villaizan, M.D. Shape-shifted red blood cells: A novel red blood cell stage? *Cells* **2018**, *7*, 31. [[CrossRef](#)]
18. Puente-Marin, S.; Nombela, I.; Ciordia, S.; Mena, M.C.; Chico, V.; Coll, J.; Ortega-Villaizan, M.D.M. In silico functional networks identified in fish nucleated red blood cells by means of transcriptomic and proteomic profiling. *Genes* **2018**, *9*, 202. [[CrossRef](#)]
19. Hong, C.S.; Funk, S.; Muller, L.; Boyiadzis, M.; Whiteside, T. Isolation of biologically active and morphologically intact exosomes from plasma of patients with cancer. *J. Extracell. Vesicles* **2016**, *5*, 29289. [[CrossRef](#)]
20. Liu, S.; Chen, J.; Shi, J.; Zhou, W.; Wang, L.; Fang, W.; Zhong, Y.; Chen, X.; Chen, Y.; Sabri, A.; et al. M1-like macrophage-derived exosomes suppress angiogenesis and exacerbate cardiac dysfunction in a myocardial infarction microenvironment. *Basic Res. Cardiol.* **2020**, *115*, 22. [[CrossRef](#)]
21. Nikapitiya, C.; Chandrarathna, H.P.S.U.; Dananjaya, S.H.S.; De Zoysa, M. Isolation and characterization of phage (ETP-1) specific to multidrug resistant pathogenic *Edwardsiella tarda* and its in vivo biocontrol efficacy in zebrafish (*Danio rerio*). *Biologicals* **2020**, *63*, 14–23. [[CrossRef](#)] [[PubMed](#)]
22. Welch, J.L.; Madison, M.N.; Margolick, J.B.; Galvin, S.; Gupta, P.; Martínez-Maz, O.; Dash, C.; Okeoma, C.M. Effect of prolonged freezing of semen on exosome recovery and biologic activity. *Sci. Rep.* **2017**, *7*, 45034. [[CrossRef](#)] [[PubMed](#)]
23. Livak, K.J.; Schmittgen, T.D. Analysis of relative gene expression data using real time quantitative PCR and the $2^{-\Delta\Delta CT}$ method. *Methods* **2001**, *25*, 402–408. [[CrossRef](#)] [[PubMed](#)]
24. Cheng, K.; Escalon, B.L.; Robert, J.; Chinchar, V.G.; Reyer, N.G. Differential transcription of fathead minnow immune-related genes following infection with frog virus 3, an emerging pathogen of ectothermic vertebrates. *Virology* **2014**, *456*, 77–86. [[CrossRef](#)]
25. Chen, J.; Xia, L.; Wang, W.; Wang, Z.; Hou, S.; Xie, C.; Cai, J.; Lu, Y. Identification of a mitochondrial-targeting secretory protein from *Nocardia seriolae* which induces apoptosis in fathead minnow cells. *J. Fish. Dis.* **2019**, *42*, 1493–1507. [[CrossRef](#)]
26. Wang, F.; Jiao, H.; Liu, W.; Chen, B.; Wang, Y.; Chen, B.; Lu, Y.; Su, J.; Zhang, Y.; Liu, X. The antiviral mechanism of viperin and its splice variant in spring viremia of carp virus infected fathead minnow cells. *Fish. Shellfish Immunol.* **2019**, *86*, 805–813. [[CrossRef](#)]
27. Rikkert, L.G.; Nieuwland, R.; Terstappen, L.; Terstappen, L.W.M.M.; Coumans, F.A.W. Quality extracellular vesicle images by transmission electron microscopy is operator and protocol dependent. *Extracell. Vesicles* **2019**, *8*, 1555419. [[CrossRef](#)]
28. Chuo, S.T.Y.; Cheien, J.C.Y.; Lai, C.P.K. Imaging extracellular vesicles: Current and emerging methods. *J. Biomed. Sci.* **2018**, *25*, 91. [[CrossRef](#)]
29. Kim, Y.S.; Ahn, J.S.; Kim, S.; Kim, H.J.; Kim, S.H.; Kang, J.S. The potential theragnostic (diagnostic therapeutic) application of exosomes in diverse biomedical fields. *Korean J. Physiol. Pharmacol.* **2018**, *22*, 113–125. [[CrossRef](#)]
30. Patel, G.K.; Khan, M.A.; Zubair, H.; Srivastava, S.K.; Khushman, M.; Singh, S.; Singh, A.P. Comparative analysis of exosome isolation methods using culture supernatant for optimum yield, purity and downstream applications. *Sci. Rep.* **2019**, *9*, 5335. [[CrossRef](#)]
31. Ding, X.Q.; Wang, Z.Y.; Xia, D.; Wang, R.X.; Pan, X.R.; Tong, J.H. Proteomic profiling of serum exosomes from patients with metastatic gastric cancer. *Front. Oncol.* **2020**, *10*, 1113. [[CrossRef](#)] [[PubMed](#)]
32. Enderle, D.; Spiel, A.; Coticchia, C.M.; Berghoff, E.; Mueller, R.; Schlumpberger, M.; Sprenger-Haussels, M.; Shaffer, J.M.; Lader, E.; Skog, J.; et al. Characterization of RNA from exosomes and other extracellular vesicles isolated by a novel spin column-based method. *PLoS ONE* **2015**, *10*, e0136133. [[CrossRef](#)] [[PubMed](#)]
33. Gutiérrez García, G.; Galicia García, G.; Zalapa Soto, J.; Izquierdo Medina, A.; Rotzinger-Rodríguez, M.; Casas Aguilar, G.A.; López Pacheco, C.P.; Aguayo, Á.; Aguilar-Hernandez, M.M. Analysis of RNA yield in extracellular vesicles isolated by membrane affinity column and differential ultracentrifugation. *PLoS ONE* **2020**, *6*, e0238545. [[CrossRef](#)] [[PubMed](#)]
34. Baranyai, T.; Herczeg, K.; Onódi, Z.; Voszka, I.; Módos, K.; Marton, N.; Nagy, G.; Mäger, I.; Wood, M.J.; El Andaloussi, S.; et al. Isolation of exosomes from blood plasma: Qualitative and quantitative comparison of ultracentrifugation and size exclusion chromatography methods. *PLoS ONE* **2015**, *10*, e0145686. [[CrossRef](#)] [[PubMed](#)]
35. Gorr, T.A.; Vogel, J. Western blotting revisited: Critical perusal of underappreciated technical issues. *Proteomics Clin. Appl.* **2015**, *9*, 396–405. [[CrossRef](#)]

36. Ryu, K.J.; Lee, J.Y.; Park, C.; Cho, D.; Kim, S.J. Isolation of small extracellular vesicles from human serum using a combination of ultracentrifugation with polymer-based precipitation. *Ann. Lab. Med.* **2020**, *40*, 253–258. [[CrossRef](#)]
37. McDonald, M.K.; Tian, Y.; Qureshi, R.A.; Gormley, M.; Ertel, A.; Gao, R.; Lopez, E.A.; Alexander, G.M.; Sacan, A.; Fortina, P.; et al. Functional significance of macrophage-derived exosomes in inflammation and pain. *Pain* **2014**, *155*, 1527–1539. [[CrossRef](#)]
38. Tarbes, S.M.; Borrás, F.E.; Montoya, M.; Fraile, L.; Portillo, H.A.D. Serum-derived exosomes from non-viremic animals previously exposed to the porcine respiratory and reproductive virus contain antigenic viral proteins. *Veter. Res.* **2016**, *47*, 59. [[CrossRef](#)]
39. Zhu, X.; Badawi, M.; Pomeroy, S.; Sutaria, D.S.; Xie, Z.; Baek, A.; Jiang, J.; Elgamal, O.A.; Mo, X.; Perle, K.L.; et al. Comprehensive toxicity and immunogenicity studies reveal minimal effects in mice following sustained dosing of extracellular vesicles derived from HEK293T cells. *J. Extracell. Vesic.* **2017**, *6*, 1324730. [[CrossRef](#)]